since 1961

Baltica

BALTICA Volume 34 Number 1 June 2021: 1–16
https://doi.org/10.5200/baltica.2021.1.1

Evidence of ice streaming and ice tongue shutdown in western Latvia: revealed from the mapping of crevasse-squeeze ridges

Kristaps Lamsters*, Zane Vītola, Jānis Karušs, Pēteris Džeriņš

Lamsters, K., Karušs, J., Vītola, Z., Džeriņs, P. 2021. Evidence of ice streaming and ice tongue shutdown in western Latvia: revealed from the mapping of crevasse-squeeze ridges, *Baltica, 34 (1)*, 1–16. Vilnius. ISSN 0067-3064.
Manuscript submitted 27 October 2020 / Accepted 21 April 2021 / Available online 20 June 2021

Abstract. Glacial geomorphological mapping of western Latvia using a 1-m-resolution digital elevation model generated from airborne LiDAR data has revealed two sets of mega-scale glacial lineations (MSGLs), one of which is superimposed by crevasse-squeeze ridges (CSRs). CSRs occur as a dense ridge network with a dominant orientation of ridges perpendicular to the ice flow direction. The landform assemblage is interpreted as evidence for two separate phases of fast ice flow with different ice flow directions during the overall deglaciation of the Fennoscandian Ice Sheet (FIS). The first fast ice flow phase occurred from the northwest by the Usma Ice Lobe that extended in the Eastern Kursa Upland. The second fast ice flow occurred from the north by the Venta Ice Tongue in a narrow flow corridor limited mainly to the Kursa Lowland. Active ice streaming caused ice crevassing perpendicular to the ice flow direction and formation of CSRs by squeezing of subglacial till into basal crevasses. A good preservation of the CSRs and general lack of recessional moraines suggest widespread stagnation and ice mass melting after the shutdown of the Venta Ice Tongue followed by the formation of the Venta-Usma ice-dammed lake and glaciolacustrine deposition in the lowest areas of lowland. Our data provide the first evidence of CSRs in the south-eastern terrestrial sector of the FIS suggesting the dynamic ice streaming or surging behaviour of the ice lobes and tongues in this region during deglaciation.

Keywords: *surge; fast ice flow; subglacial bedforms; MSGL; basal crevasses*

✉ *Kristaps Lamsters* (kristaps.lamsters@lu.lv), Zane Vītola (zane.vitola3@inbox.lv), Jānis Karušs (janis.karush@lu.lv), Pēteris Džeriņš (peteris.dzerins@lu.lv), University of Latvia, Faculty of Geography and Earth Sciences, Jelgavas Str. 1, LV-1004, Riga, Latvia*
**Corresponding author at University of Latvia, Faculty of Geography and Earth Sciences, Jelgavas Str. 1, LV-1004, Riga, Latvia. Email: kristaps.lamsters@lu.lv*

INTRODUCTION

Geometrical (rectilinear) ridge networks represented as crevasse squeeze ridges (CSRs) are widely distributed at the forelands of surging glaciers (e.g. Evans, Rea 1999; Rea, Evans 2011; Schomacker *et al.* 2014; Flink *et al.* 2015; Ingólfsson *et al.* 2016; Aradóttir *et al.* 2019) and have been regarded as diagnostic landforms of glacier surging for a long while (e.g. Sharp 1985a, b), although Evans, Rea (2003) have noted that "they cannot be regarded independently as diagnostic features of palaeo-glacier surging even though widespread development of crevasse-squeeze networks clearly requires extensive fracturing of the glacier, normally associated with surging".

Furthermore, CSRs have been used to infer glacier dynamics and especially the surging or fast ice streaming of both modern glaciers (e.g. Farnsworth *et al.* 2016) and paleo-ice streams and lobes of the Laurentide (Evans *et al.* 1999, 2008, 2016, 2020; Ankerstjerne *et al.* 2015; Cline 2011; Cline *et al.* 2015), Fennoscandian (Greenwood *et al.* 2016), Irish (Delaney *et al.* 2018), Barents Sea (Andreassen *et al.* 2014; Bjarnadóttir *et al*. 2014; Kurjanski *et al.* 2019), Patagonian Mountain (Ponce *et al.* 2019) ice sheets and even Antarctic inter-ice stream areas (Klages *et* *al.* 2013). The availability of high-resolution digital elevation models (DEMs) produced from LiDAR data has rapidly increased the recognition and mapping of CSRs at the paleo-ice stream beds during the recent years (see references above) thus facilitating their usage for diagnosing ice streaming (e.g. Evans *et al.* 2008, 2016) or surging (e.g. Evans *et al.* 1999, 2020; Ankerstjerne *et al.* 2015; Cline *et al.* 2015; Delaney *et al.* 2018; Ponce *et al.* 2019) considering the possible modern analogous landsystems of surging glaciers (Evans, Rea 1999, 2003) and active temperate glacier lobes (Evans *et al.* 2015).

A distinct surge behaviour has not been documented for any contemporary ice streams (Cuffey, Paterson 2010; Sevestre, Benn 2015), except in the case of a potential surge or ice streaming event of the Kamb Ice Stream, West Antarctica in the past (Engelhardt, Kamb 2013), the past switch in ice stream flow directions from the Ross Sea sector of West Antarctica (Conway *et al.* 2002) and speed-ups or surges of the glaciers after the collapse of the Larsen A and B Ice Shelves of the Antarctic Peninsula (De Angelis, Skvarca 2003). The only reported observation of an ice stream being formed was from the destabilized Vavilov Ice Cap with ice flow rates exceeding 1 km per year (Zheng *et al.* 2019). These rare observations, however, are supported by results of physical experiments that have demonstrated the potential of ice streams to switch on and off emphasising their dynamic behaviour and dependence on subglacial drainage (Lelandais *et al.* 2018).

CSRs have been often mapped in close association with mega-scale glacial lineations (MSGLs), which are widely accepted as characteristic landforms of fast ice flow and are used for the identification of ice stream tracks (e.g. Clark 1993; Stokes, Clark 2002; Stokes *et al.* 2013; Spagnolo *et al*. 2014; Ely *et al.* 2016). In this study we aim to map CSRs and MSGLs of the Venta Ice Tongue (VIT) that operated in western Latvia at the final stages of the deglaciation of the Fennoscandian Ice Sheet (FIS) (Zelčs, Markots 2004) and to analyse the morphological characteristics and internal structure of CSRs to confirm their origin. The LiDAR-based mapping allows not only the recognition and mapping of previously unknown subglacial landforms but furthermore they provide useful insights into the dynamics of ice streaming/surging in western Latvia.

MATERIALS AND METHODS

Study area

Our study area is located in the Kursa Lowland and adjoining part of the Eastern Kursa Upland in western Latvia (Fig. 1). The bedrock in this area consists of Upper Devonian terrigenous and carbonaceous rocks of varied composition that are distributed as narrow bands of SW-NE orientation thus becoming younger in the southern direction. The bedrock surface lies over 100 m a.s.l. at the Eastern Kursa Upland and decrease to 0 m a.s.l. at the SE corner of the lowland. The central and southern part of the lowland is located on the bedrock slope inclined to the west. The bedrock both at the Kursa Lowland and the Eastern Kursa Upland is overlain by a thin cover (10–20 m) of Quaternary sediments that reaches a maximum thickness of only 30 m in the north-western part of the area. In the western part of the Kursa Lowland and the western and northern parts of Eastern Kursa Upland, the cover of Quaternary sediments is even less than 10 m. Quaternary sediments consist mainly of Late Weichselian till underlain by glaciofluvial sediments in places and overlain by a thin (few meters) cover of glaciolacustrine sediments (sand, silt, clay). The glaciolacustrine sediments cover the majority of the Kursa Lowland, except the eastern part, and were deposited in the Venta-Usma ice-dammed lake, which developed during the North Lithuanian glacial phase (Zelčs, Markots 2004) approximately 15 ka ago (Stroeven *et al.* 2016). Occasionally, small patches of till occur between glaciolacustrine sediments. Only in some lower depressions and bedrock incisions, possible remains of Saalian till have been noted (Juškevičs *et al.* 1999).

At the time of the Late Weichselian glaciation, western Latvia was covered by the Baltic Ice Stream (BIS) of the FIS. During the course of deglaciation, the BIS, the flow direction of which was generally from north, divided into the Usma and Kursa ice lobes (Fig. 1) that were additionally split in several local ice tongues. The southernmost extension of the UIL was the VIT that converged in the Kursa Lowland during the late deglaciation (Zelčs, Markots 2004).

The glacial geomorphology of the study area has been historically investigated mainly at the Eastern Kursa Upland (Straume 1979; Strautnieks 1998; Kalnina *et al.* 2007). The NW-SE oriented convergent drumlins were described from the NW part of the Upland as the Vāne drumlin field, and the transverse (W–E) oriented ridges from the W part of the Upland were interpreted as De Geer moraines forming the Vārme-Zirņu DeGeer moraine field (Strautnieks 1998). This field occupies the tilted plain that gradually stretches into the Kursa Lowland. In this study the genesis of these small transverse ridges is re-interpreted. The historically drawn border between lowland and upland areas is not clearly defined in the topography, although the lateral margins of the VIT are well-expressed on the airborne LiDAR DEM (Fig. 1.) Thus, the VIT operated partially also on the western part of the Eastern Kursa Upland.

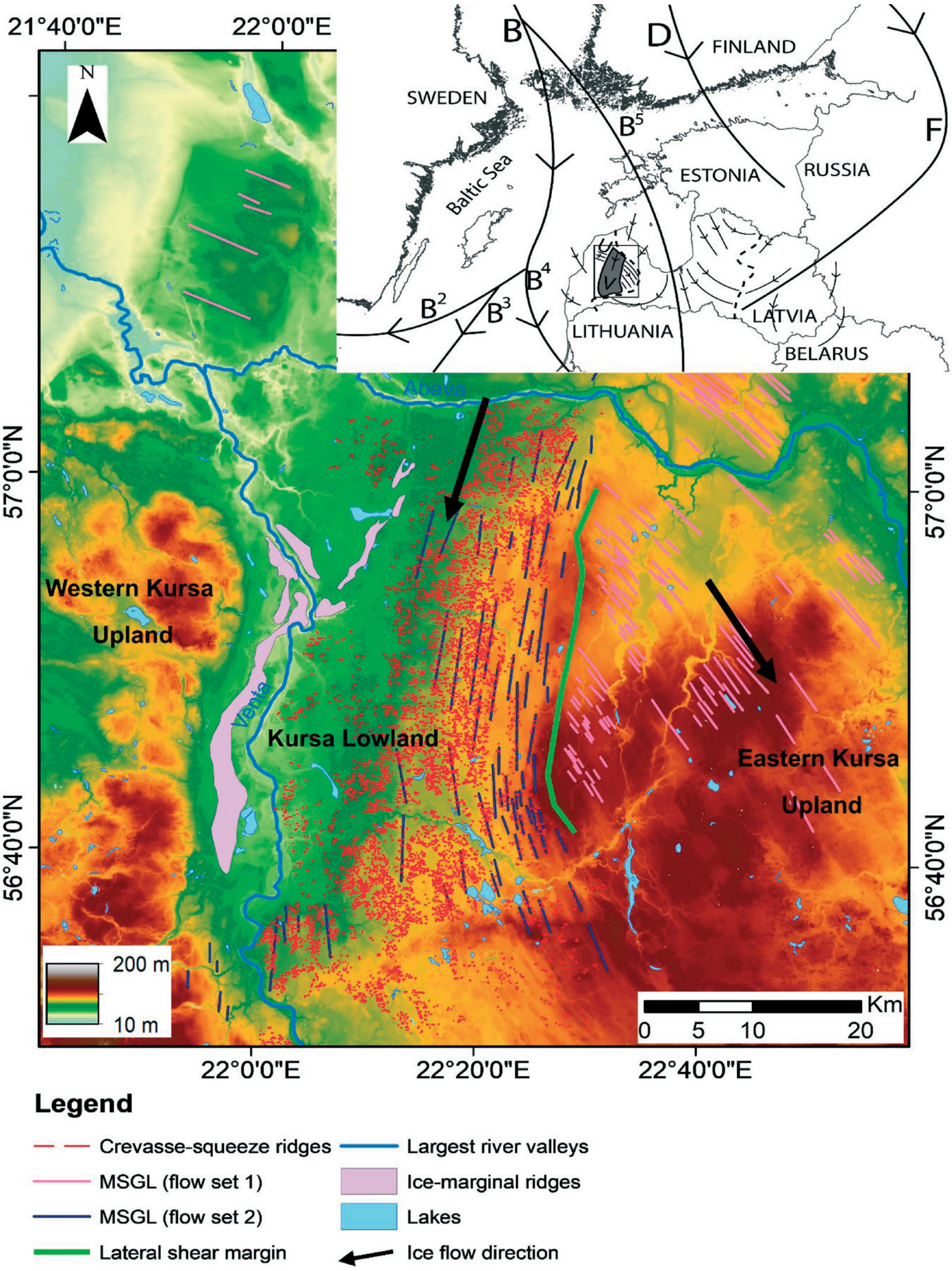

Fig. 1 Relief-shaded DEM of the study area in the western Latvia with mapped CSRs and MSGLs. Ice streams in the inset map are modified after Boulton *et al*. (2001) and Kalm (2012). Smaller flowlines correspond to ice lobes and tongues after Zelčs, Markots (2004). The location of Venta ice tongue (V) and flowlines of Usma ice lobe (U) is determined from this study. B – Baltic ice stream complex with Kursa lobe (Kursian after Zelčs, Markots 2004 or Neman stream after Kalm 2012) (B4) and Riga (B5) ice-streams. D – Peipsi–Pskov ice stream. F – Ladoga–Ilmen–Lovat' ice stream

METHODS

The geomorphological mapping was performed from the 1-m-resolution airborne LiDAR-based DEM (Fig. 1) available as a raster file from the Latvian Geospatial Information Agency. The mapping was done in ArcMap software digitizing the crests of subglacial bedforms as lines. The LiDAR DEM was displayed by applying a shaded relief function thus enhancing the visibility of landforms.

The geological structure of CSRs was determined using geological drilling and Electrical Resistivity Tomography (ERT). Drilling was performed by hand auger, and altogether 13 boreholes were drilled in the survey area up to the depth of 6 m. The boreholes were drilled in the CSRs at several locations across the Kursa Lowland. One CSR at the southern part of the Lowland was investigated in detail. Three boreholes were drilled across the ridge, and two pits with dimensions of 1 × 1 m were excavated. The structure of sediments was studied in both pits together with measurements of till macrofabric, which were performed on the horizontal surface more than 50 cm from the ground surface, measuring the orientation of the longest axis of elongated pebbles.

As till sediments are almost impenetrable for the electromagnetic waves (Neal 2004) produced by a ground penetrating radar, we used ERT survey to characterize the sediments in the CSRs and below them. ERT survey was carried out using a multichannel *Syscal Pro Switch* (*IRIS Instruments*) device. Measurements were performed with 72 stainless steel electrodes and by using Schlumberger electrode configuration (Reynolds 1997) with 2 m separation between electrodes. Overall, 2 ERT profiles, each 142 m long, were placed parallel and transverse on the CSR. The location of each of the electrodes was measured using an RTK GNSS device. Before the ERT measurements, contact resistance of each electrode with the ground was measured. Results showed low resistivities (< 2 kOhm*m), which corresponds to a good contact with the ground and a considerably small signal loss.

ERT data processing was carried out using *Geotomo Res2DInv* 3.5 software (Loke 2004). The first step of data processing was to manually check for any outliers. The signal that corresponds to resistivity values of the ground changes gradually; therefore, any data points that noticeably differ from surrounding points are likely to indicate problems with electrode contact with the ground during the measurements or caused by near-surface in homogeneities (Mohamed 2006). In this survey, no outliers were found. The least-squares inversion of apparent resistivity data was carried out using the Quasi-Newton method (Loke, Barker 1996). For the inversion process, the finite-element mesh was used. The resulting models were topographically corrected to account for elevation changes along the profile. Further, both models were exported to *ParaView* software (version 5.8.1.) for 3D visualization using linear contour intervals. As obtained data showed low resistivities and small changes in it across the whole investigated depth, colour scale was adjusted (40 to 110 Ohm*m) so that it is more sensitive towards small changes in low resistivities, neglecting extremely high values which are of less interest.

RESULTS AND INTERPRETATION

Geomorphology

We have identified and mapped an assemblage of subglacial landforms at the Kursa Lowland and Eastern Kursa Upland in the western Latvia that we interpret mainly as MSGLs and CSRs (Figs 1–2). The identified MSGLs have two main orientations and we divide them into two separate flow sets (Fig. 2). The first flow set crosses the Eastern Kursa Lowland, and crests of landforms are oriented in the NW-SE direction (pink flow set in Figs 1 and 2). They consist of at least 130 parallel, elongated ridges with a typical amplitude of a few meters and width of a few hundred meters. Their maximum height is 9 m, while the lengths of individual segments usually vary from 1 to 7 km. The shorter lengths are mainly a result of postglacial fluvial erosion, where rivers crosscut ridge crests, thereby dividing them into shorter segments. If such segments are connected, the possible true length of some MSGLs reaches 17 km and elongation ratios reach several tens of meters. Some ridges are even narrower than 100 m and can be classified as megaflutings. The ice-disintegration features cover the MSGLs in places. The second set of elongated ridges (blue flow set in Figs 1 and 2) is mainly located at the western part of the Eastern Kursa Upland and eastern part of the Kursa Lowland and postdates the first set. These ridges have a N-S orientation in general, which changes from NNE–SSW in the north to NNW–SSE in the south as a result of the ice flow bending along the slope of the Eastern Kursa Upland. Similar to the ridges of the first flow set, their length varies from 1 to 10 km with a few ridges possibly extending up to 15 km, and their widths are a few hundred up to 800 meters. Their true length is not easily measured because the ridges usually have a low amplitude of a few meters and in places are covered by glaciolacustrine sediments and superimposed by numerous transverse ridges. The shortest but also the highest (up to 15 m) ridges occur at the southern part of the lowland and SW corner of the Eastern Kursa Upland.

Based on the similarity of the described ridges to elongated landforms identified at paleo-ice stream beds around the globe (e.g. Clark 1993; Stokes, Clark 2002; Ó Cofaigh *et al*. 2013; Stokes *et al.* 2013; Spagnolo *et al*. 2014; Lamsters, Zelčs 2015; Ely *et al.* 2016), we interpret the majority of them as MSGLs, consistent with the formation under a fast flowing ice lobe or ice tongue. Some shorter ridges and some narrower ones could also be classified as megaflutings and drumlins, which are often found at the same paleo-ice stream (lobe) beds forming a continuum of streamlined subglacial bedforms (lineations) (e.g. Ely *et al*. 2016).

We attribute the two sets of MSGLs to two fast ice flow phases. The first phase occurred from NW by the UIL that extended in the area of the Eastern Kursa Upland. The second ice flow phase occurred later by the VIT in a narrow flow corridor limited mainly to the Kursa Lowland, where the ice flow was generally from north. This ice flow completely destroyed any landforms that may possibly have developed during the first flow phase in the Kursa Lowland. The VIT was laterally topographically confined by the Western Kursa Upland in the west and a lateral shear margin in the east (Fig. 2). Based on the existing regional reconstructions (Zelčs, Markots 2004; Zelčs *et al.* 2011; Kalm 2012), we attribute the first flow set to the Middle Lithuanian (locally – Gulbene) glacial phase at ~16 ka and the second flow set to the North Lithuanian (locally – Linkuva) glacial phase at ~15 ka (Stroeven *et al.* 2016). The Linkuva ice-marginal position is marked by the ice-marginal ridge in the western side of the Kursa Lowland, and the eastern margin of the VIT is clearly represented by a later shear margin (Figs 1, 2). Eastward of the shear margin, the older set of NW-SE oriented MSGLs is visible. The southern limit of the VIT is marked by the Pampāļi Interlobate Ridge (Fig. 2). The ice-margin position during the Linkuva phase was drawn to the north of the Pampāļi Interlobate Ridge by Zelčs *et al.* (2011); however, this study does not reveal any other ice-marginal formations north of the Pampāļi Ridge. Also, the record of CSRs suggests the presence of an ice tongue up to the Pampāļi Ridge. The newest Valdemārpils glacial phase is marked in the central western side of the Kursa Lowland (Zelčs *et al.* 2011). The possible southernmost position of the Valdemārpils glacial phase can be traced by ice-marginal ridges (Fig. 2); however, the eastern position is questionable and cannot be marked precisely.

A total of 7067 small rectilinear ridges were mapped in the Kursa lowland, within the topographic low hosting MSGL flow set 2 (Figs 1–2). We interpret the rectilinear ridges as CSRs based on their resemblance to and common characteristics with such ridges revealed in numerous investigations at modern and paleo-ice stream and/or ice lobe beds (Sharp 1985a, b; Evans, Rea 1999, 2003; Evans *et al.* 1999, 2008, 2016, 2020; Rea, Evans 2011; Andreassen *et al.* 2014; Bjarnadóttir *et al.* 2014; Schomacker *et al.* 2014; Ankerstjerne *et al.* 2015; Cline *et al.* 2015; Flink *et al.* 2015; Farnsworth *et al.* 2016; Greenwood *et al.* 2016; Ingólfsson *et al.* 2016; Delaney *et al.* 2018; Aradóttir *et al.* 2019; Kurjanski *et al.* 2019; Ponce *et al.* 2019). Measurements of the orientation of the crests of CSRs reveal a dominant W–E alignment (Fig. 2) reflecting transverse ice fractures during their formation, although other variations exist as well, for example, a system of NNE–SSW, WNW–ESE and W–E oriented ridges occur in close proximity to each other (Fig. 3A). The regional ice flow direction in the Kursa Lowland is determined from the orientation of MSGLs that follow N–S alignment in general. The lengths of individual CSRs are mainly between 150 and 300 m (Fig. 4) with a mean length of 219 m. Only a few CSRs exceed the length of 600 m, and none of the mapped CSRs are shorter than 50 m. The crest heights of CSRs range from only a few tens of centimetres to 8 m at maximum but are typically 1–2 m high. The majority of ridge slopes are symmetrical (Fig. 4). The ridges are generally straight or very slightly arcuate (Fig. 3B). The ridges are typically around 30–80 m wide, although small, narrower ridges are also relatively common. A handful of the largest and longest ridges reach the maximum width of almost 300 m.

In general, CSRs have a low preservation potential due to their low amplitude. They are prone to postglacial disintegration, forming minor sediment hummocks that display no preferred orientation (e.g. Sutherland *et al.* 2019). Where such hummocks occur in close association with other CSRs, we interpret them to be collapsed and not well-preserved CSRs. The distance between individual ridges varies (along the ice flow direction). Often, a very dense network of ridges occurs where the width of ridges is similar to the distance between them (Fig. 3C).

The mapped CSRs continue over a distance of 80 km over the entire VIT bed up to the Pampāļi Interlobate Ridge (Fig. 2) that developed between the fronts of the southward flowing VIT and northwestward flowing Vadakste Ice Tongue (Lamsters, Zelčs 2015). The southernmost limit of the CSRs is not exactly at the Pampāļi Ridge, as some CSRs are visible on its opposite side as well and could be related to the stagnation of the Vadakste Ice Tongue. The maximum width of the CSRs cover is 30 km, but it diminishes in the central part of their distribution area because the majority of the Kursa lowland is covered by glaciolacustrine sediments (Fig. 3) (Straume 1979; Juškevičs *et al.* 1999), which effectively mask low amplitude CSRs. Only the higher ones or those located on topographical elevations are still visible on the plain of the Venta-Usma ice-dammed lake. The westernmost limit of possible CSRs coincides with a wide valley of the Venta River (Fig. 3).

Internal structure

The internal structure of CSRs was inspected by field analyses of 13 boreholes drilled at several sites across the study area. All drilled boreholes revealed that investigated CSRs consist completely of glacial till that only differs by colour or grain size from site to site and is represented as clayey silty sand or silty sandy clay with pebbles (Fig. 5). The colour of till is characterized by various shades of brown. The composition of one CSR was further investigated in detail by drilling three boreholes (Fig. 6) and digging two pits at the ridge crest and slope. The central borehole reveals a 5-m-thick reddish-brown till bed underlain by violet-brown and light grey till. Two other boreholes drilled at the slopes of the ridge have slightly more clayey till that is underlain by grey till as well. The majority of these boreholes run deeper than the

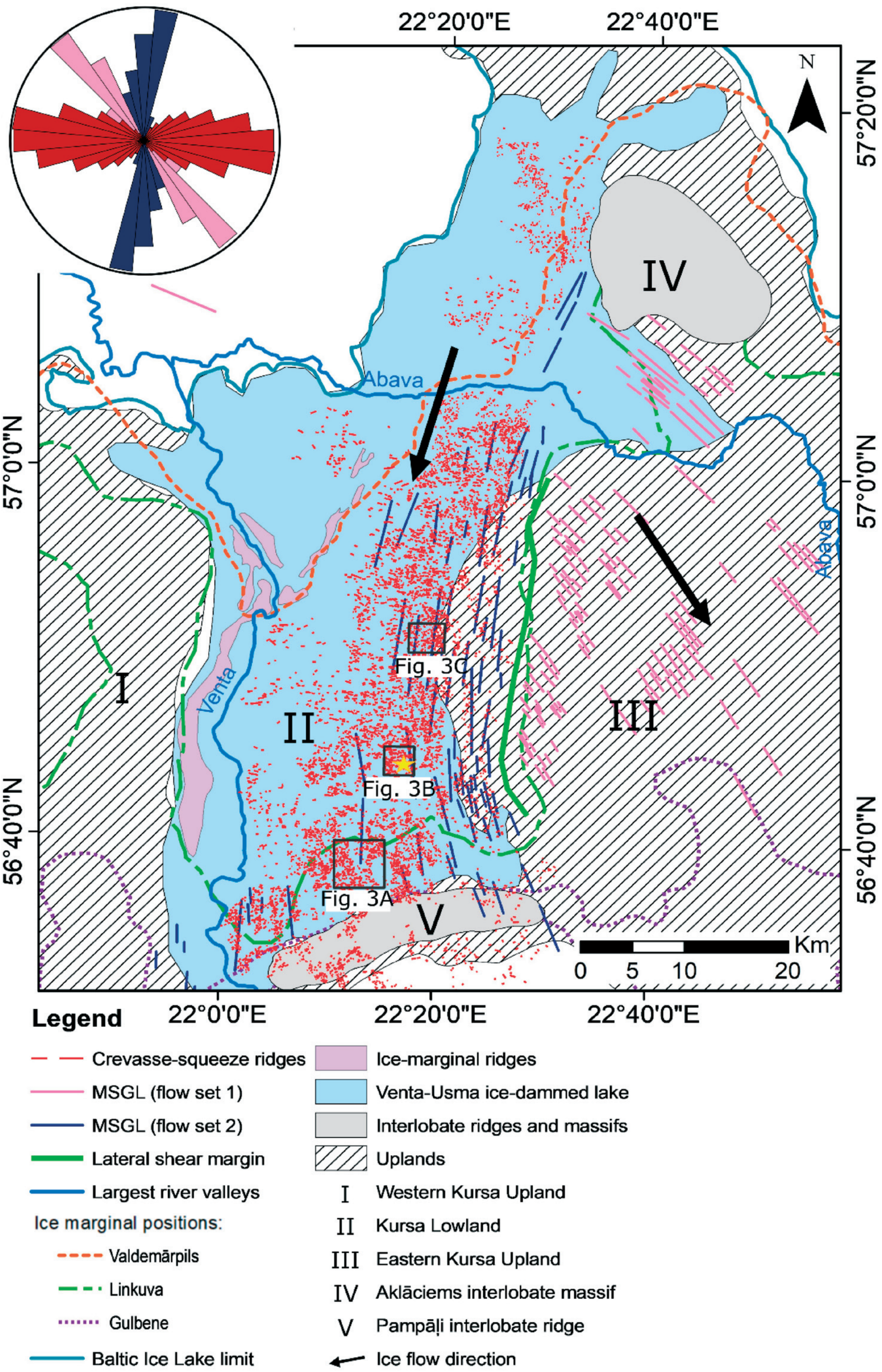

Fig. 2 Glacial geomorphological map of the Kursa Lowland and adjoining upland areas showing the mapped glacigenic landforms. The rose diagram shows the orientation of the crests of crevasse-squeeze ridges (red) and MSGLs of the VIT (blue) and UIL (purple). The ice-marginal positions are from Zelčs *et al*. (2011). Yellow star – the location of the studied CSR shown in Fig. 6

ridge itself. Thus, they do not only expose the structure of the CSR but also reveal older till that was possibly deposited during the main advance of the BIS.

A homogenous matrix-supported till was revealed in both pits without any internal deformation. The compactness of till and bullet-shaped form of polished pebbles suggest a subglacial origin. Fabrics are moderately clustered with S1 eigenvalues ranging from 0.56 to 0.59, indicating relatively low strains. No visible till fissility was observed, further implying low shear stress that would be appropriate for a saturated material being squeezed in a crevasse. The azimuth of maximum clustering as indicated by V1 eigenvector (199) at the ridge crest is parallel to the regional ice

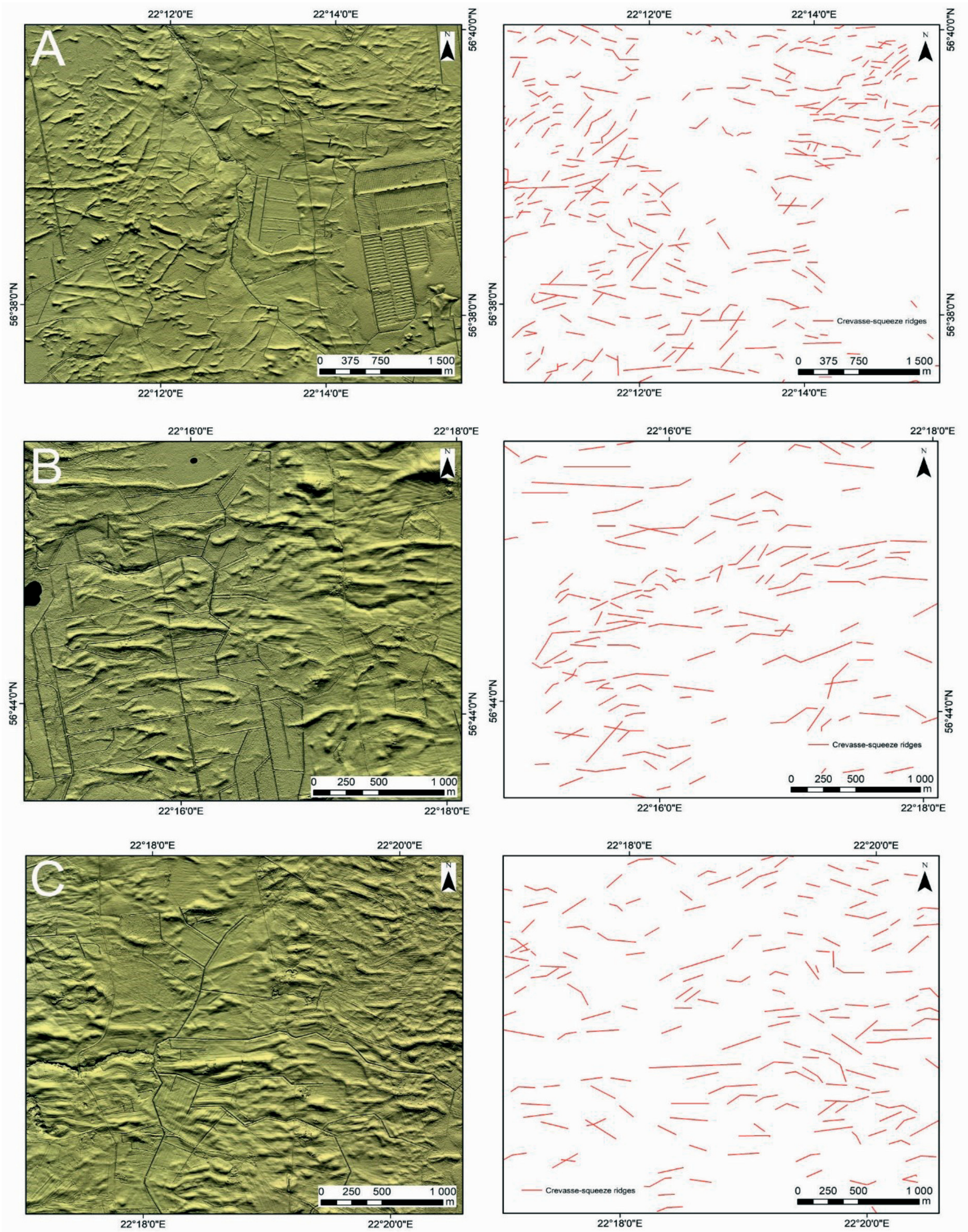

Fig. 3 Close-ups of DEMs and interpreted CSRs. A: Several systems of differently orientated CSRs. B: Long, W–E oriented CSRs. C: A very dense network of small CSRs

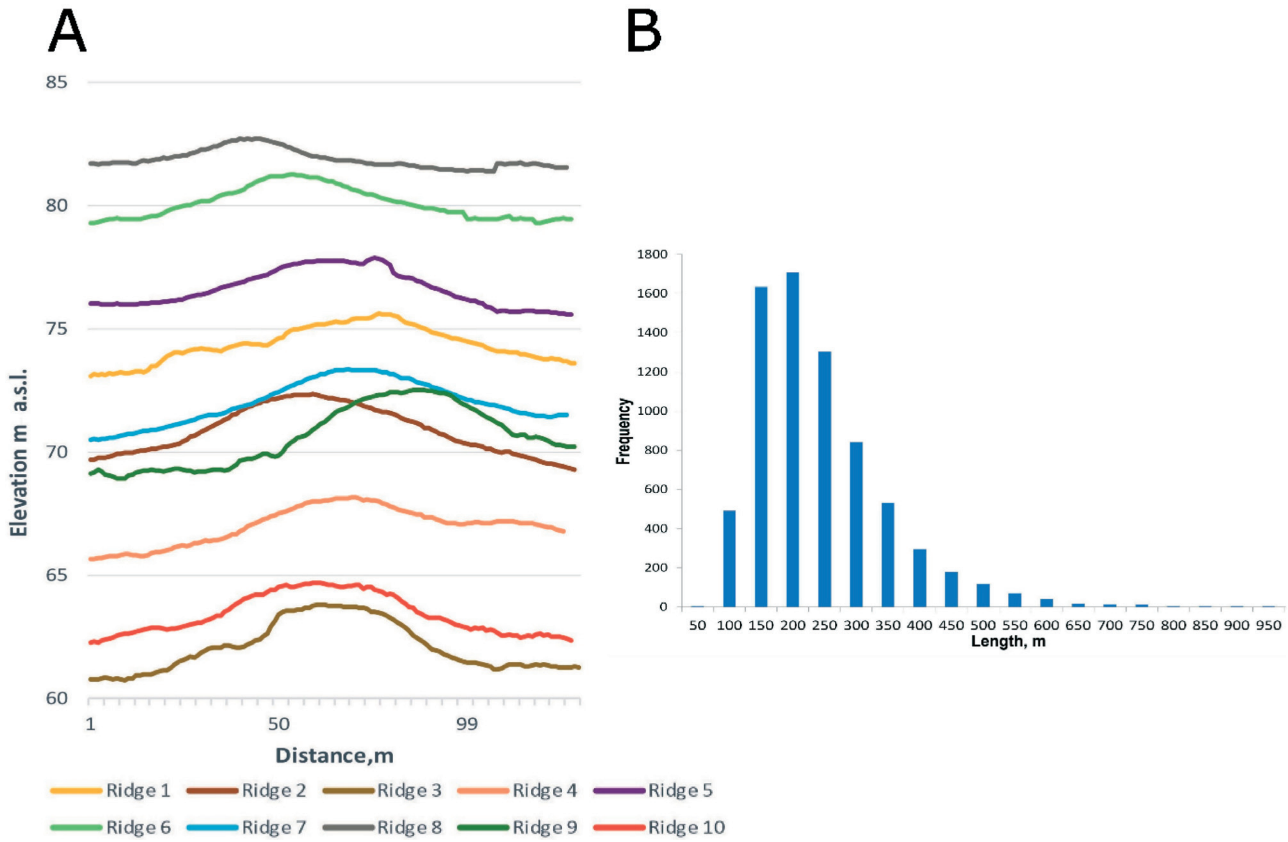

Fig. 4 A. The topographic cross-sections of randomly chosen CSRs parallel to ice flow direction across the entire distribution area. B. The distribution of length of the mapped CSRs

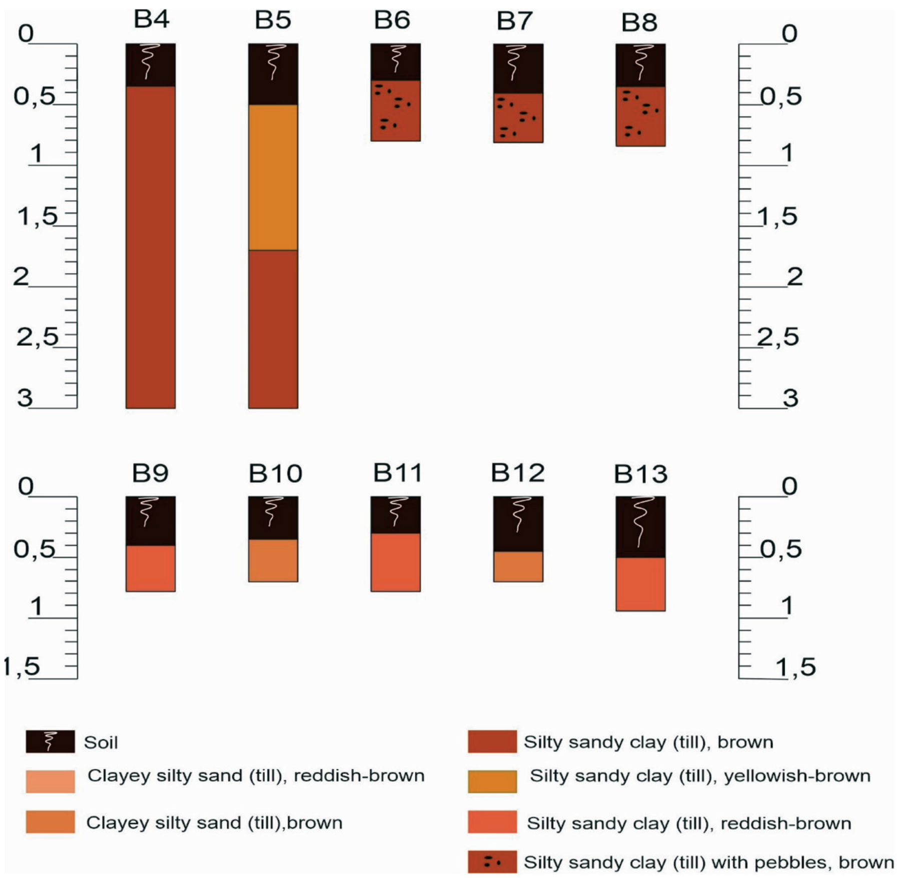

Fig. 5 The composition of CSRs from boreholes

flow direction from NNE and forms a narrow angle with the orientation of the ridge crest segment, which in this place is not transverse to the ice flow direction. Many clasts are very steeply dipping (some being completely vertical) with the average dip angle of 44 degrees. Such high clast dip angles have previously been described for CSRs (Sharp 1985a, b; Evans, Rea 2003; Evans *et al*. 2020), indicating the subglacial till emplacement direction from the glacier bed into a basal or full-depth crevasse. Fabrics at the second measurement site at the ridge foot are different and have V1 eigenvector of 118 degrees but this is based only on the measurement of 19 clasts due to a very poor content of pebbles in a till. The main difference is the dip angle of clasts, which is considerably lower (average – 22), thus supporting the assumption that clasts at the ridge crest tend to plunge more steeply due to the squeezing of till in the glacier crevasse.

Two ERT profiles were recorded parallel and perpendicular to the previously mentioned CSR. They reveal a mainly twofold structure of the investigated geological section (Fig. 7). The upper part can be distinguished as a separate layer of approximate thickness of 6 m and it is very homogenous and characterized by low resistivity values. The lower part of the section has slightly higher resistivity values. Although resistivity values are similar, it is possible to distinguish the upper layer across the entire profile. Profile 2, which was recorded parallel to the ridge crest shows very little resistivity variations throughout the profile. Especially homogenous are the uppermost 6 m implying that the electrical properties of the material forming the CSR do not vary either vertically or laterally. We interpret the upper layer as till, which was verified by drilling. The lower part of the section is interpreted as bedrock that, according to the description of boreholes in this area made by the State Geological Survey, is close to the ground surface (Juškevičs *et al*. 1999). As each of these boreholes reveal different sedimentary rock types, ranging from clay and sand to domerite, it is not possible to ascertain the rock type below the particular CSRs; however, the electrical resistivity values indicate that this should be clayey material.

Profile 1, which was recorded perpendicular to the ridge crest, reveals more variations of resistivity values (although they are still very similar), especially close to the surface. On both sides of the CSR there

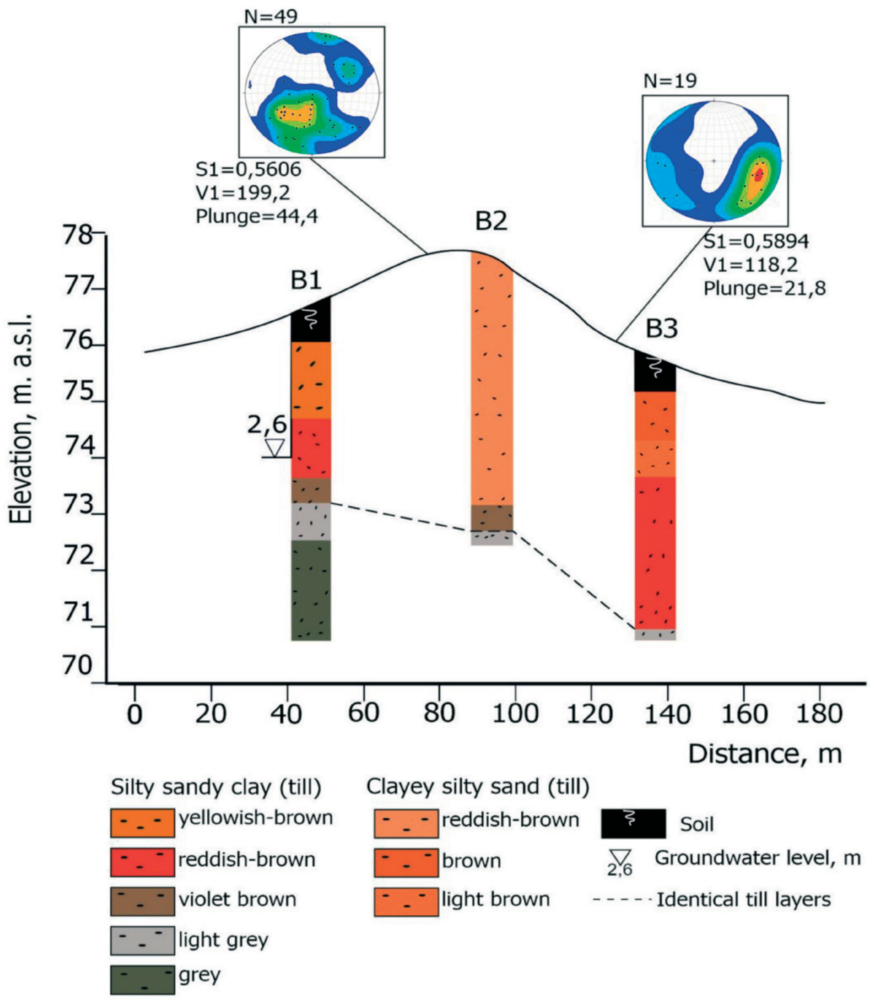

Fig. 6 The composition and till fabrics of the CSR investigated in details. See location in Fig. 2

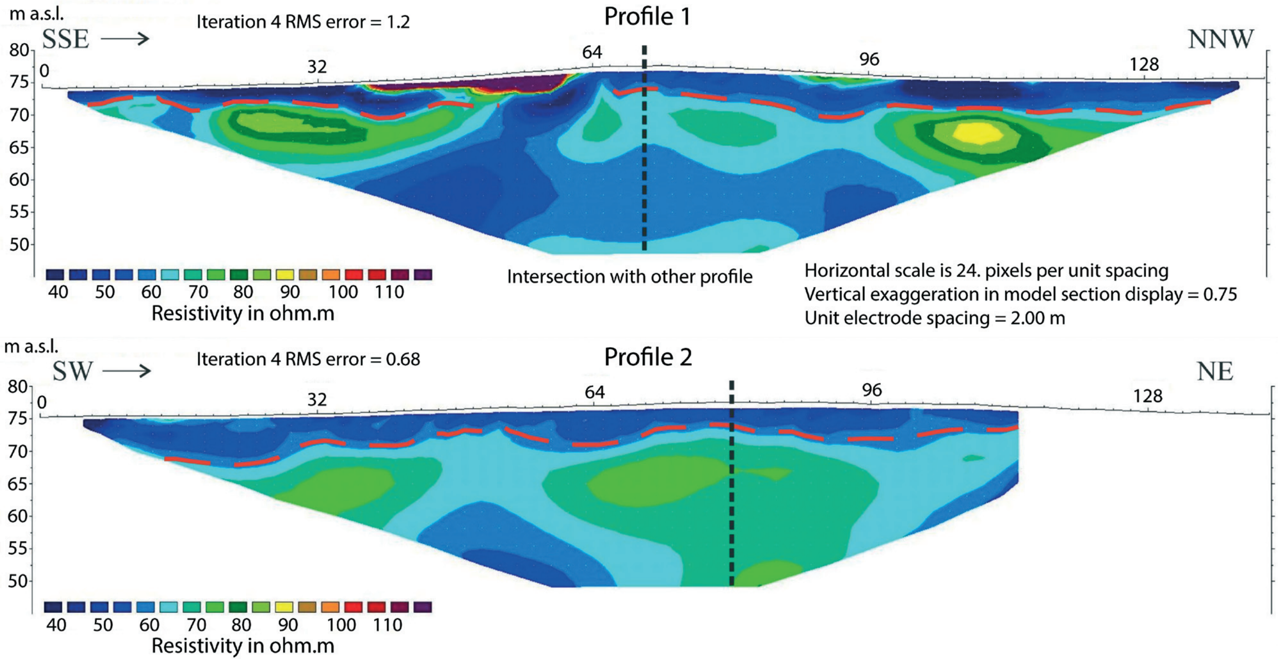

Fig. 7 ERT profiles at the CSR. Profile 1 is transverse and Profile 2 is parallel to the crest of CSR. Northeast end of Profile 2 is cut out due to problems during data acquisition

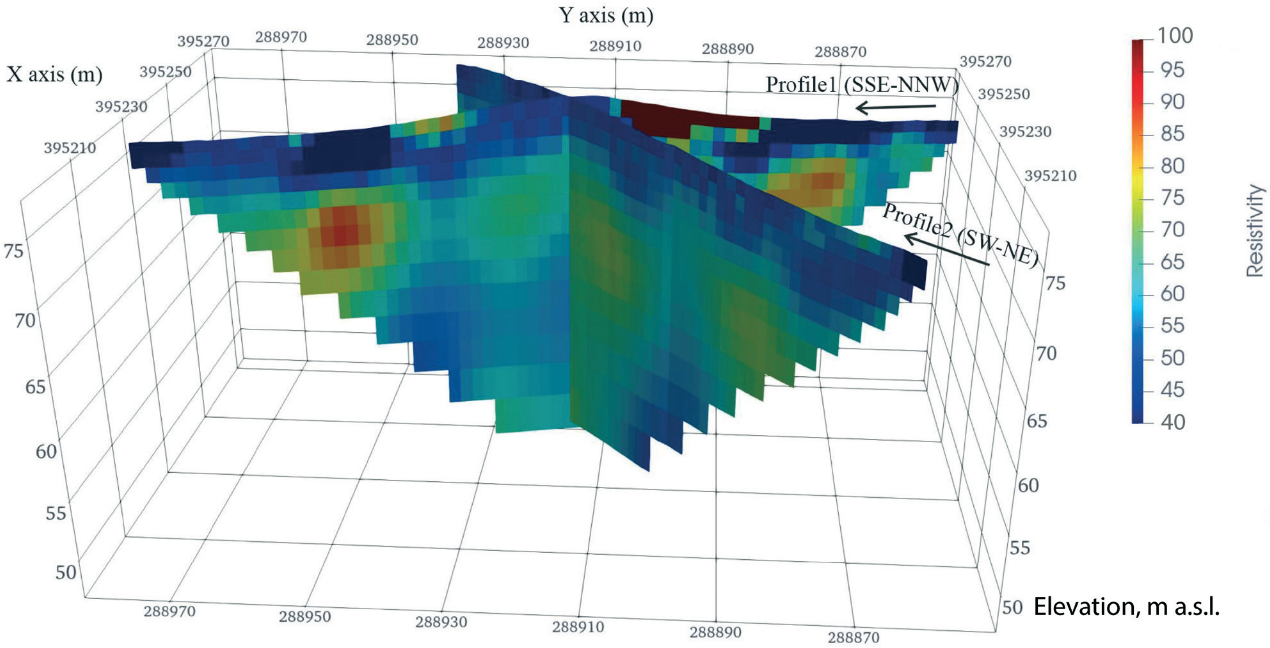

Fig. 8 Combined ERT 3D profile

are areas of higher electrical resistivity. To better evaluate the compatibility of both ERT profiles and the structure of the CSR, both profiles were joined and visualised in a 3D model (Fig. 8). As expected, both ERT profiles show approximately the same thickness of the low-resistivity upper layer in their cross-section. Figure 8 further illustrates that high resistivity zones close to the surface are distributed on both sides of the CSR. Although it is not possible to explain the source of these higher resistivity anomalies with certainty based on our data, one possible explanation could be changes of granulometric composition, moisture or amount of organic matter. At the ridge crest, the entire soil cover was washed down and accumulated as colluvium material at the slopes of the CSR. However, given the size of these anomalies, local inhomogenities related to the CSR structure cannot be excluded as a possible source.

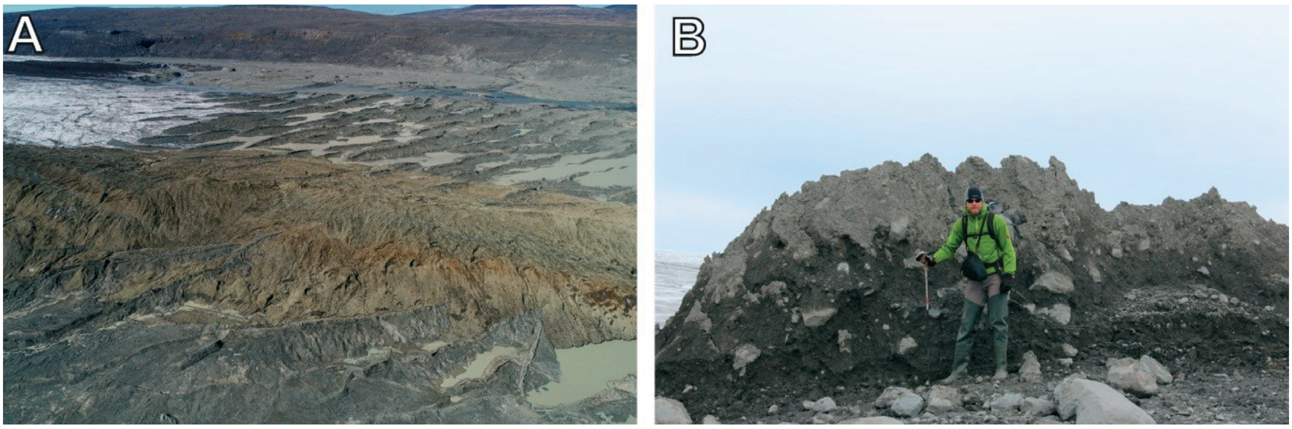

Fig. 9 The modern examples of CSRs in Iceland. A: CSRs melting from the margin of the Eyjabakkajökull glacier. Ice flow from left to right. The prominent feature stretching across the image is a medial moraine. Note also CSRs melting form englacial position. B: Freshly deposited and ice-cored CSR with very steep slopes at the margin of Thjórsárjökull

DISCUSSION

The described assemblage of subglacial landforms is unique in the south-eastern sector of the FIS, as CSRs have not been previously reported from this region and are mainly known from marine-based ice streams (Greenwood *et al.* 2016) of the central sector of the FIS, except of limited mainland areas (Kleman 1988; Öhrling *et al.* 2020). However, MSGLs and flutings, which are characteristic landforms of fast ice flow (Clark 1993; Stokes, Clark 2002; Stokes *et al.* 2013; Ely *et al.* 2016), are highly typical bedforms of the fast flowing ice streams and lobes of the south-eastern (Zelčs 2000; Kalm 2012; Karmazienė *et al.* 2013; Baltrūnas *et al.* 2014, 2020; Lamsters, Zelčs 2015) and central sectors (Greenwood *et al.* 2016; Putkinen *et al.* 2017; Möller, Dowling 2018) of the FIS that developed during its overall deglaciation.

It is commonly accepted that the formation of CSRs results mainly from the infilling of basal bottom-up or full-depth crevasses and that high basal water pressures are a prerequisite for the formation of crevasses by hydrofracturing and squeezing of till into crevasses (e.g. Rea, Evans 2011). Alternatively, top-down infilling can occur by the accumulation of supraglacial debris or glaciofluvial material but this mechanism would make the preservation of CSRs less likely (Evans *et al.* 2016). The possibility of CSRs to develop from englacial debris-rich structures has been noted as well (Bennett *et al.* 1996; Evans, Rea 1999, 2003; Rea, Evans 2011; Lovell *et al.* 2015). Unfortunately, it is difficult to evaluate the possible englacial transport of sediment-filled fractures or thrust faults at the paleo-ice streams but, for example, Ankerstjerne *et al.* (2015) who did detailed analyses of the properties of sediments constructing CSRs concluded that the formation of CSRs was assisted by basal ice motion and occurred prior to complete ice stagnation during the late stages of surge. Modern examples often show ice-cored nature of freshly deposited CSRs, and melting of CSRs from englacial position as evidenced, for example, at the front of Eyjabakkajökull, Iceland (Schomacker *et al.* 2014; Lamsters *et al.* 2020) (Fig. 9).

Additionally, studies from surging glaciers in Trygghamna, West Svalbard, indicate that basal till was squeezed into basal crevasses or thrust faults through hydrofracturing during the active surge phase, elevated and transported englacially as debris-rich structures before the deposition upon surge termination (Lovell *et al.* 2015; Ben-Yehoshua 2017). Thus, it is clear that some modern examples from surging glaciers clearly advocate for englacial transport of subglacial debris before deposition, and we cannot exclude the possibility of englacial transport of some of CSRs at the VIT bed as well. A pattern of CSRs with variable orientations and no dominant alignment perpendicular to centreline ice flow direction has been observed at the Tunabreen, Svalbard, and has been suggested to reflect dominantly compressive flow, where hydrofracturing, thrust faulting, and thrust-style displacement were prevalent complicating the stress, fracture, and debris-rich structure orientations (Lovell *et al.* 2015). In general, the orientation of CSRs at the VIT bed is very distinct, suggesting mainly longitudinal extension and development of CSRs into tensional basal or full-depth crevasses. However, in the case of locally occurring complex and very dense networks made up of variably oriented cross-cutting CSRs, very small ridges and even hummocks (Fig. 3A, C), the development of englacial debris-rich structures or a complex fracture network due to locally complicated stress regimes cannot be ruled out.

The prevailing opinion is that CSRs form by injection of till into basal crevasses immediately prior to ice lobe/stream shutdown and that only little internal deformation occurs after (e.g. Evans, Rea 1999; Evans *et al.* 2016). We agree with this interpretation, because we find it impossible to explain the observed widespread distribution and good preservation of CSRs at the bed of VIT if the ice stream had remained active after their formation. The subsequent widespread stagnation and rapid mass melting and passive retreat is a prerequisite for the preservation of CSRs, otherwise they would have been destroyed or overprinted during subsequent ice advances. Such a rapid retreat of highly fractured ice without regrounding of ice body was also suggested and demonstrated from the CSRs record of the Bothnian Sea ice stream (Greenwood *et al.* 2016). Modern examples exist proving that a lack of CSRs suggests non-stagnant ice characterized by small winter re-advances during the overall retreat (Aradóttir *et al.* 2019).

The spatial patterns and regional distributions of CSR networks have been used by Evans *et al.* (1999, 2008, 2014) to propose that they form by squeezing of subglacial till into basal crevasses formed during glacier surging, as identified on modern surging glaciers (Sharp 1985a, b; Evans, Rea 1999, 2003; Evans *et al.* 2007; Schomacker, Kjær 2007). Although the majority of CSRs at contemporary glacier margins have been interpreted as diagnostic features for glacier surging (e.g. Farnsworth *et al.* 2016), some CSRs have been reported from active temperate glacier margins (Evans *et al.* 2015) as well. On the other hand, some potential surge glaciers have also been reported despite the absence of diagnostic surge-type landforms including CSRs (Aradóttir *et al.* 2019). The CSRs from active temperate glacier margins (Evans *et al.* 2015), however, are characterized mainly by a radial crevasse pattern that is distinct from the pattern of mainly transverse CSRs identified at modern surging glaciers. Such radial crevasses commonly develop at the Icelandic south coast active temperate piedmont lobes and are mainly associated with the formation of pecten/radial crevasse infillings by pushing and squeezing saturated till into the pecten that produce sawtooth moraines in non-surging snouts (Evans *et al.* 2017). The formation of distinct CSRs at such glacier lobes, however, is known from rare examples (Evans *et al.* 2015) and thus could be analogous only for paleo-ice lobes with a divergent ice flow pattern and other specific conditions.

Three CSR patterns have been reported up to now: (1) wide arcuate zones of CSRs related to widespread fracturing within glacier surge lobes, (2) narrow concentric arcs of CSRs and recessional push moraines related to submarginal till deformation at active temperate glacier lobes that experienced active ice recession, and (3) CSR corridors related to the fracturing of individual ice stream flow units (Evans *et al.* 2016). The landsystem and CSR pattern reported here does not correspond to any of these patterns. Probably, it is due to the not-so-widespread converging or more or less parallel pattern of ice tongue flow as observed here. CSRs in western Latvia are distributed almost across the entire ice tongue bed (Figs 1, 2), suggesting widespread fracturing and passive retreat later. Although the majority of CSRs are concentrated on the eastern side of the study area, we assume that some of these low-amplitude ridges are covered by glaciolacustrine sediments in the lowest elevations of the Kursa Lowland (see the distribution of the Venta-Usma ice-dammed lake in Fig. 2) and some destroyed by fluvial activity, especially in the vicinity of the Venta River valley. A thin cover of glaciolacustrine sediments underlain by till sediments was detected in some shallow boreholes in the visible CSRs as well.

The timing of paleo-surging or ice streaming of the VIT cannot be fully established from this study due to the lack of chronological evidence, but what we observe in the Kursa Lowland is one generation of MSGLs superimposed by CSRs (Fig. 2) that developed during the North Lithuanian glacial phase approximately 15 ka ago (Stroeven *et al.* 2016). Earlier generation MSGLs occur in the Eastern Kursa Upland and are most likely related to the streaming of the UIL during the Middle Lithuanian glacial phase (Zelčs, Markots 2004; Kalm 2012) ~16 ka ago (Stroeven *et al.* 2016). We attribute the mapped CSRs to an ice streaming or surging event. Such events are likely to have occurred along the southern margin of the FIS, as the latest reconstructions of the FIS have shown the highly lobated margin at 16 and 15 ka that could possibly be related to surge activity (Stroeven *et al.* 2016).

Similar events have also been reported during the retreat of the FIS in the Gulf of Bothnia, when the Bothnian Sea sector rapidly pulsed and collapsed because of the culmination of a succession of short-lived stream, surge or re-advance events (Greenwood *et al.* 2016). The idea of asynchronous surges along the south-eastern margin of the FIS was proposed already in 2012 by Bitinas (2012) who attributed kame terraces located on the distal slopes of recessional marginal ridges and plateau-like glaciolacustrine kames in Lithuania to the interaction of active ice lobes (surges) and masses of dead ice that persisted beyond the ice margin. Thus, our study complements the recognition of such fast ice flow events or surges at the southern and eastern FIS margins during deglaciation. Although the so-called surge fans, which represent strongly divergent and fast ice flow of ice streams (after Kleman *et al.* 1997), have already been proposed for the southern Finland and Bothnian Sea (Kleman *et al.* 1997; Greenwood *et al.* 2016), the surge-like behaviour of an ice tongue (laterally topographically constrained) of the south-eastern sector is clearly demonstrated for the first time. A possible surge behaviour, however, has been proposed also for the highly divergent Zemgale Ice Lobe of the Riga Ice Stream (Kleman *et al.* 1997; Bitinas 2012; Baltrūnas *et al.* 2020). The main evidence for such event could be MSGLs mapped by Lamsters, Zelčs (2015), although not emphasised by these authors as MSGLs are not considered to be characteristic landforms for surging glaciers.

However, before we call something a surge, we should remember the indication of Benn, Evans (2010) that "In some of the literature, however, the term 'surge' is used more loosely to refer to any dramatic glacier speed-up". Bearing this in mind, it would not be adequate to call the advance of the VIT a surge event because we do not have any supporting evidence showing that this was a sudden and short-lived fast ice flow acceleration following a period of slow flow (quiescent phase), which is the definition of glacier surges (Dowdeswell *et al.* 1991; Benn, Evans 2010). It was emphasised also by Margold *et al.* (2018) who reconstructed ice stream activity during the deglaciation of the Laurentide Ice Sheet and noted (with reference to Raymond 1987) that "the fan-shaped ice stream track likely indicates a one-off fast ice flow event (in the literature on the regional glacial history often called a surge, even though a surging glacier sensu stricto should undergo repeated periods of advance and quiescence". It is worth to pay attention also to the notion that potential fast flow events had usually been associated to fan-shaped ice streams (Margold *et al.* 2018) but the VIT was characterized by ice flow convergence. Ice streaming contrary to surging is characterized by long-lasting fast ice flow known from modern Antarctic ice streams producing streamlined landforms including MSGL (King *et al.* 2009; Davies *et al.* 2018) and exhibiting dynamic behaviour that could possibly result in ice stream switch off and on and change of ice flow directions as observed in Antarctica (Conway *et al.* 2002; Engelhardt, Kamb 2013). Whether we can call ice stream speed-up events surges, it is still an open question.

The intense fracturing of the VIT responsible for the development of CSRs could be attributed to fast ice flow (streaming) producing mainly the longitudinal tensile strain regime. Fast ice flow is also clearly evidenced by the MSGLs, the lengths of which sometimes exceed 10 km. Prerequisites for fast ice flow possibly were a combination of topographic factors (previously eroded and deepened lowland) and a thin cover of soft and easily erodible sediments underlain by sedimentary bedrock of comparatively lower water permeability (Juškevičs *et al.* 1999.). Ice streaming occurred until a rapid shutdown of the VIT because there is no other landform record of transverse ridges indicative of slower ice flow speeds or possible steady-state normal–fast flow (Evans *et al.* 2014) that could follow the streaming phase. There is also no record of recessional moraines that could develop if active ice recession took place. The formation of CSRs most probably occurred immediately after the active streaming phase but prior to the ice tongue shutdown when basal water pressures were reduced to a point sustaining ice-bed coupling. Yet, the basal water pressure still remained sufficiently large to facilitate squeezing of saturated subglacial till into basal and/or full-depth crevasses. After ice flow ceased, the widespread stagnation and rapid retreat of ice took place. Such widespread retreat and mass melting, which is largely sustained by ice surface melting and thinning or the so-called areal deglaciation, has been proposed as the main ice retreat component in Lithuania as well (Bitinas 2012). Thus, wider implications of the discovery of CSRs on the VIT bed are related to possible ice streaming or surging events at the south-eastern sector of the FIS during overall deglaciation followed by ice stagnation and rapid mass melting afterwards. Such events could be even more widespread than previously thought, and this should be considered in further reconstructions of FIS deglaciation considering both fast ice flow or surge events and widespread stagnation generating large bodies of ice-dammed lakes.

CONCLUSIONS

In this study, we have recognized and mapped an assemblage of subglacial landforms in western Latvia consisting of two sets of MSGLs and one set of CSRs from high-resolution (1 m) DEM generated from airborne LiDAR data. A dense network of small rectilinear and transverse ridges occurring on and between MSGLs developed during the second fast flow phase and are interpreted as CSRs formed by subglacial till squeezing into basal or full-depth crevasses immediately prior the shutdown of the VIT. This is supported by the composition of ridges investigated in two test pits, boreholes and by ERT. In all cases, CSRs consist of homogenous glacial till. The two sets of MSGLs indicate two phases of fast ice flow with different ice flow directions during the overall deglaciation of the FIS. The first fast ice flow phase by the UIL was from NW and is related to the Middle Lithuanian glacial phase at ~16 ka but the second fast ice flow phase was from N by the VIT and is related to the North Lithuanian glacial phase at ~15 ka. The active ice streaming or surging event that created mainly transverse crevasses due to a high longitudinal tensile stress was followed by widespread ice lobe stagnation after the second phase of active ice flow as suggested from the good preservation of CSRs and their distribution pattern.

Here, we have provided the first evidence of CSRs in the south-eastern terrestrial sector of the FIS, thereby also adding to the overall knowledge of CSR distribution worldwide. Together with CSRs, which have previously been recognised at modern glaciers and in paleo-ice stream records, we have interpreted them as an indication of ice streaming events or surge-like behaviour during the deglaciation of the FIS.

ACKNOWLEDGEMENTS

This work was financially supported by the specific support objective activity 1.1.1.2. "Post-doctoral Research Aid" (Project id. N. 1.1.1.2/16/I/001) of the Republic of Latvia, funded by the European Regional Development Fund, PostDoc Kristaps Lamsters research project No. 1.1.1.2/VIAA/1/16/118 and by performance-based funding of the University of Latvia within the "Climate change and sustainable use of natural resources" programme. We thank two anonymous reviewers for valuable comments and suggestions.

REFERENCES

Andreassen, K., Winsborrow, M.C., Bjarnadóttir, L.R. and Rüther, D.C. 2014. Ice stream retreat dynamics inferred from an assemblage of landforms in the northern Barents Sea. *Quaternary Science Reviews 92*, 246–257.

Ankerstjerne, S., Iverson, N.R., Lagroix, F. 2015. Origin of a washboard moraine of the Des Moines Lobe inferred from sediment properties. *Geomorphology 248*, 452–463.

Aradóttir, N., Ingólfsson, Ó., Noormets, R., Benediktsson, Í.Ö., Ben-Yehoshua, D., Håkansson, L., Schomacker, A. 2019. Glacial geomorphology of Trygghamna, western Svalbard-Integrating terrestrial and submarine archives for a better understanding of past glacial dynamics. *Geomorphology 344*, 75–89.

Baltrūnas, V., Waller, R.I., Kazakauskas, V., Paškauskas,S., Katinas, V. 2014. A comparative case study of subglacial bedforms in northern Lithuania and south-eastern Iceland. *Baltica 27 (2)*, 75–92.

Baltrūnas, V., Karmaza, B., Katinas, V., Pukelytė, V., Karmazienė, D., Lozovskis, S. 2020. Till macro- and microfabrics of mega-scale glacial lineations of Mūša–Nemunėlis Lowland, north Lithuania. *Baltica 33 (1)*, 85–96.

Benn, D.I., Evans, D.J.A. 2010. *Glaciers and Glaciation*. Second edition. Hodder Education, London, 802 pp.

Bennett, M.R., Hambrey, M.J., Huddart, D., Ghienne, J.F. 1996. The formation of a geometrical ridge network by the surge-type glacier Kongsvegen, Svalbard. *Journal of Quaternary Science 11 (6)*, 437–449.

Ben-Yehoshua, D. 2017. Crevasse-Squeeze Ridges in Trygghamna, Svalbard. *MSc. Thesis*, University of Iceland, Reykjavik, 164 pp.

Bitinas, A. 2012. New insights into the last deglaciation of the south-eastern flank of the Scandinavian Ice Sheet. *Quaternary Science Reviews 44*, 69–80.

Bjarnadóttir, L.R., Winsborrow, M.C.M., Andreassen, K. 2014. Deglaciation of the central Barents Sea. *Quaternary Science Reviews 92*, 208–226.

Boulton, G.S., Dongelmans, P., Punkari, M., Broadgate, M. 2001. Palaeoglaciology of an ice sheet through a glacial cycle: the European ice sheet through the Weichselian. *Quaternary Science Reviews 20 (4)*, 591–625.

Clark, C.D. 1993. Mega-scale glacial lineations and cross-cutting ice flow landforms. *Earth Surface Processes and Landforms 18*, 1–29.

Cline, M.D. 2011. Spatial analysis of Des Moines Lobe washboard moraines using LiDAR data. *Graduate Theses and Dissertations*, Iowa State University, 10387.

Cline, M.D., Iverson, N.R., Harding, C. 2015. Origin of washboard moraines of the Des Moines Lobe: Spatial analyses with LiDAR data. *Geomorphology 246*, 570–578.

Conway, H., Catania, G., Raymond, C.F., Gades, A.M., Scambos, T.A., Engelhardt, H. 2002. Switch of flow direction in an Antarctic ice stream. *Nature 419* (*6906*), 465–467.

Cuffey, K.M., Paterson, W.S.B. 2010. *The physics of glaciers*. Fourth edition. Academic Press, Amsterdam, etc., 704 pp.

Davies, D., Bingham, R.G., King, E.C., Smith, A.M., Brisbourne, A.M., Spagnolo, M., Graham, A.G., Hogg, A.E., Vaughan, D.G. 2018. How dynamic are ice-stream beds? *The Cryosphere 12*, 1615–1628.

De Angelis, H., Skvarca, P. 2003. Glacier surge after ice shelf collapse. *Science 299 (5612)*, 1560–1562.

Delaney, C.A., McCarron, S., Davis, S. 2018. Irish Ice Sheet dynamics during deglaciation of the central Irish Midlands: evidence of ice streaming and surging from airborne LiDAR. *Geomorphology 306*, 235–253.

Dowdeswell, J.A., Hamilton, G.S., Hagen, J.O. 1991. The duration of the active phase on surge-type glaciers: Contrasts between Svalbard and other regions. *Journal of Glaciology 37 (127),* 388–400.

Ely, J.C., Clark, C.D., Spagnolo, M., Stokes, C.R., Greenwood, S.L., Hughes, A.L.C., Dunlop, P., Hess, D. 2016. Do subglacial bedforms comprise a size and shape continuum? *Geomorphology 257*, 108–119.

Engelhardt, H., Kamb, B. 2013. Kamb Ice Stream flow history and surge potential. *Annals of Glaciology 54 (63)*, 287–298.

Evans, D.J.A., Rea, B.R. 1999. Geomorphology and sedimentology of surging glaciers: a landsystem approach. *Annals of Glaciology 28*, 75–82.

Evans, D.J.A., Rea, B.R. 2003. Surging glacier landsystem. In: Evans, D.J.A. (ed.), Glacial Landsystems. Arnold, London, 259–288, https://doi.org/10.4324/9780203784976

Evans, D.J.A., Lemmen, D.S., Rea, B.R. 1999. Glacial landsystems of the southwest Laurentide Ice Sheet: modern Icelandic analogues. *Journal of Quaternary Science 14* 673–691.

Evans, D.J.A., Twigg, D.R., Rea, B.R., Shand, M. 2007. Surficial geology and geomorphology of the Brúar-

jökull surging glacier landsystem. *Journal of Maps 3 (1)*, 349–367.
Evans, D.J., Clark, C.D., Rea, B.R. 2008. Landform and sediment imprints of fast glacier flow in the southwest Laurentide Ice Sheet. *Journal of Quaternary Science 23 (3)*, 249–272.
Evans, D.J., Young, N.J., Cofaigh, C.Ó. 2014. Glacial geomorphology of terrestrial-terminating fast flow lobes/ice stream margins in the southwest Laurentide Ice Sheet. *Geomorphology 204*, 86–113.
Evans, D.J.A., Ewertowski, M., Orton, C. 2015. Fláajökull (north lobe), Iceland: active temperate piedmont lobe glacial landsystem. *Journal of Maps 12 (5)*, 77–789.
Evans, D.J., Storrar, R.D., Rea, B.R. 2016. Crevasse-squeeze ridge corridors: diagnostic features of late-stage palaeo-ice stream activity. *Geomorphology 258*, 40–50.
Evans, D.J., Ewertowski, M., Orton, C. 2017. Skaftafellsjökull, Iceland: glacial geomorphology recording glacier recession since the Little Ice Age. *Journal of Maps 13 (2)*, 358–368.
Evans, D.J., Atkinson, N., Phillips, E. 2020. Glacial geomorphology of the Neutral Hills Uplands, southeast Alberta, Canada: The process-form imprints of dynamic ice streams and surging ice lobes. Geomorphology 350, 106910, https://doi.org/10.1016/j.geomorph.2019.106910
Farnsworth, W.R., Ingólfsson, Ó., Retelle, M., Schomacker, A. 2016. Over 400 previously undocumented Svalbard surge-type glaciers identified. *Geomorphology 264*, 52–60.
Flink, A.E., Noormets, R., Kirchner, N., Benn, D.I., Luckman, A., Lovell, H. 2015. The evolution of a submarine landform record following recent and multiple surges of Tunabreen glacier, Svalbard. *Quaternary Science Reviews 108*, 37–50.
Greenwood, S.L., Clason, C.C., Nyberg, J., Jakobsson, M., Holmlund, P. 2016. The Bothnian Sea ice stream: early Holocene retreat dynamics of the south-central Fennoscandian Ice Sheet. *Boreas 46 (2)*, 346–362.
Ingólfsson, Ó., Benediktsson, Í.Ö., Schomacker, A., Kjær, K.H., Brynjólfsson, S., Jonsson, S.A., Korsgaard, N.J., Johnson, M.D. 2016. Glacial geological studies of surge-type glaciers in Iceland–Research status and future challenges. *Earth-Science Reviews 152*, 37–69.
Juškevičs, V., Mūrnieks, A., Misāns, J. 1999. Geological map of Latvia, scale 1:200,000. Sheet 42 – Jūrmala. *Explanatory Notes and Maps*. O. Āboltiņš, V. Kuršs (eds). State Geological Survey, Riga. [In Latvian with English summary].
Kalm, V. 2012. Ice-flow pattern and extent of the last Scandinavian Ice Sheet southeast of the Baltic Sea. *Quaternary Science Reviews 44*, 51–59.
Kalnina, L., Strautnieks, I., Cerina, A. 2007. Upper Pleistocene biostratigraphy and traces of glaciotectonics at the Satiki site, western Latvia. *Quaternary International 164*, 197–206.
Karmazienė, D., Karmaza, B., Baltrūnas, V. 2013. Glacial geology of North Lithuanian ice marginal ridge and surrounding plains. *Baltica 26 (1),* 57–70.
King, E.C., Hindmarsh, R.C.A., Stokes, C.R. 2009. Formation of mega-scale glacial lineations observed beneath a West Antarctic ice stream. *Nature Geoscience 2*, 585–588.
Klages, J.P., Kuhn, G., Hillenbrand, C.D., Graham, A.G.C., Smith, J.A., Larter, R.D., Gohl, K. 2013. First geomorphological record and glacial history of an inter-ice stream ridge on the West Antarctic continental shelf. *Quaternary Science Reviews 61*, 47–61.
Kleman, J. 1988. Linear till ridges in the southern Norwegian-Swedish mountains – evidence for a subglacial origin. *Geografiska Annaler*: *Series A, Physical Geography 70 (1–2)*, 35–45.
Kleman, J., Hättestrand, C., Borgström, I., Stroeven, A. 1997. Fennoscandian palaeoglaciology reconstructed using a glacial geological inversion model. *Journal of glaciology 43 (144)*, 283–299.
Kurjanski, B., Rea, B.R., Spagnolo, M., Winsborrow, M., Cornwell, D.G., Andreassen, K., Howell, J. 2019. Morphological evidence for marine ice stream shutdown, central Barents Sea. *Marine Geology 414*, 64–76.
Lamsters, K., Zelčs, V. 2015. Subglacial bedforms of the Zemgale Ice Lobe, SE Baltic. *Quaternary International 386*, 42–54.
Lamsters, K., Karušs, J., Krievāns, M., Ješkins, J. 2020. The thermal structure, subglacial topography and surface structures of the NE outlet of Eyjabakkajökull, east Iceland. Polar Science 100566, https://doi.org/10.1016/j.polar.2020.100566
Lelandais, T., Ravier, E., Pochat, S., Bourgeois, O., Clark, C.D., Mourgues, R., Strzerzynski, P. 2018. Modelled subglacial floods and tunnel valleys control the life cycle of transitory ice streams. *The Cryosphere 12*, 2759–2772.
Loke, M.H. 2004. Tutorial: 2-D and 3-D electrical imaging surveys. *Geotomo software, Res2dinv 3.5 software*, 136 pp.
Loke, M.H., Barker, R.D. 1996. Rapid Least-Squares Inversion of Apparent Resistivity Pseudosections Using a Quasi-Newton Method. *Geophysical Prospecting 44*, 131–152.
Lovell, H., Fleming, E.J., Benn, D.I., Hubbard, B., Lukas, S., Rea, B.R., Noormets, R., Flink, A.E. 2015. Debris entrainment and landform genesis during tidewater glacier surges. *Journal of Geophysical Research: Earth Surface 120 (8)*, 1574–1595.
Margold, M., Stokes, C.R., Clark, C.D. 2018. Reconciling records of ice streaming and ice margin retreat to produce a palaeogeographic reconstruction of the deglaciation of the Laurentide Ice Sheet. *Quaternary Science Reviews 189*, 1–30.
Mohamed, A.M.O. 2006. *Principles and Applications of Time Domain Electrometry in Geoenvironmental Engineering*. Taylor & Francis, London, 622 pp.
Möller, P., Dowling, T.P. 2018. Equifinality in glacial geomorphology: instability theory examined via ribbed

moraine and drumlins in Sweden. *GFF 140 (2)*, 106–135.
Neal, A. 2004. Ground-penetrating radar and its use in sedimentology: principles, problems and progress. *Earth-Science Reviews 66*, 261–330.
Ó Cofaigh, C., Stokes, C.R., Lian, O.B., Clark, C.D., Tulacyzk, S. 2013. Formation of mega-scale lineations on the Dubawnt Lake Ice Stream bed: 2. Sedimentology and stratigraphy. *Quaternary Science Reviews 77*, 210–227.
Öhrling, C., Peterson, G., Johnson, M.D. 2020 Glacial geomorphology between Lake Vänern and Lake Vättern, southern Sweden. *Journal of Maps 16 (2)*, 776–789.
Ponce, J.F., Guillot, M.G., Balocchi, L.D., Martínez, O. 2019. Geomorphological evidences of paleosurge activity in Lake Viedma Lobe, Patagonia, Argentina. *Geomorphology 327*, 511–522.
Putkinen, N., Eyles, N., Putkinen, S., Ojala, A.E.K., Palmu, J.P., Sarala, P., Väänänen, T., Räisänen, J., Saarelainen, J., Ahtonen, N., Rönty, H., Kiiskinen, A., Rauhaniemi, T., Tervo, T. 2017. High resolution LiDAR mapping of glacial landforms and ice stream lobes in Finland. *Bulletin of the Geological Society of Finland 89*, 64–81.
Raymond, C.F. 1987. How do glaciers surge? A review. *Journal of Geophysical Research: Solid Earth 92 (B9)*, 9121–9134.
Rea, B.R., Evans, D.J. 2011. An assessment of surge-induced crevassing and the formation of crevasse squeeze ridges. Journal of Geophysical Research: Earth Surface 116 (F4), https://doi.org/10.1029/2011JF001970
Reynolds, J. 1997. *An Introduction to Applied and Environmental Geophysics*. Wiley, New York, 806 pp.
Schomacker, A., Kjær, K.H. 2007. Origin and de-icing of multiple generations of ice-cored moraines at Brúarjökull, Iceland. *Boreas 36 (4)*, 411–425.
Schomacker, A., Benediktsson I.Ö., Ingólfsson, Ó. 2014. The Eyjabakkajökull glacial landsystem, Iceland: Geomorphic impact of multiple surges. *Geomorphology 218*, 98–107.
Sevestre, H., Benn, D.I. 2015. Climatic and geometric controls on the global distribution of surge-type glaciers: Implications for a unifying model of surging. *Journal of Glaciology 61 (228)*, 646–662.
Sharp, M. 1985a. Sedimentation and stratigraphy at Eyjabakkajökull – an Icelandic surging glacier. *Quaternary Research 24 (3)*, 268–284.
Sharp, M. 1985b. "Crevasse-fill" ridges–a landform type characteristic of surging glaciers? *Geografiska Annaler: Series A, Physical Geography 67 (3–4)*, 213–220.
Spagnolo, M., Clark, C.D., Ely, J.C., Stokes, C.R., Anderson, J.B., Andreassen, K., Graham, A.G.C., King, E.C. 2014. Size, shape and spatial arrangement of mega-scale glacial lineations from a large and diverse dataset. *Earth surface processes and landforms 39*, 1432–1448.
Stokes, C., Clark, C.D. 2002. Are long subglacial bedforms indicative of fast ice flow? *Boreas 31*, 239–249.
Stokes, C.R., Spagnolo, M., Clark, C.D., Tulaczyk, S.M., Ó Cofaigh, C., Lian, O., Dunstone, R.B. 2013. Formation of Mega-scale Glacial Lineations on the Dubawnt Lake Ice Stream bed: 1. Size, Shape and Spacing from a Large Remote Sensing Dataset. *Quaternary Science Reviews 77*, 190–209.
Straume, J. 1979. Geomorfologiya [Geomorphology]. In: Misans, J., Brangulis, A., Danilans, I., Kuršs, V. (eds) *Geologicheskoye stroyeniye i poleznyje iskopayemye Latvii*. Zinātne, Rīga, 297–439. [In Russian].
Strautnieks, I. 1998. Glacigenic landforms of the Eastern-Kursa upland and their genesis. *Dissertation work Summary*. University of Latvia, The Habilitation and Promotion Council of Geological Sciences, Rīga.
Stroeven, A.P., Hättestrand, C., Kleman, J., Heyman, J., Fabel, D., Fredin, O., Goodfellow, B.W., Harbor, J.M., Jansen, J.D., Olsen, L., Caffee, M.W. 2016. Deglaciation of Fennoscandia. *Quaternary Science Reviews 147*, 91–121.
Sutherland, J.L., Carrivick, J.L., Evans, D.J., Shulmeister, J., Quincey, D.J. 2019. The Tekapo Glacier, New Zealand, during the Last Glacial Maximum: An active temperate glacier influenced by intermittent surge activity. *Geomorphology 343*, 183–210.
Zelčs, V. 2000. Morphology, internal structure and origin of megascale flute ridges and glacial lineations in East Latvian Lowlands. In: *International Field Symposium of the Peribaltic Group and the INQUA Commission on Glaciation on Quaternary Geology in Denmark, August 29–September 3, 2000*, 56–58.
Zelčs, V., Markots, A. 2004. Deglaciation history of Latvia. In: Ehlers, J., Gibbard, P.L. (eds). *Quaternary glaciations – extent and chronology of glaciations, part I: Europe. Developments in Quaternary Science, 2*. Elsevier, Rotterdam, 225–244.
Zelčs, V., Markots, A., Nartišs, M., Saks, T. 2011. Pleistocene glaciations in Latvia. In: Ehlers, J., Gibbard, P.L., Hughes, P.D. (eds) *Developments in Quaternary Science, 15*, Elsevier, 221–229.
Zheng, W., Pritchard, M.E., Willis, M.J., Stearns, L.A. 2019. The Possible Transition From Glacial Surge to Ice Stream on Vavilov Ice Cap. *Geophysical Research Letters 46 (23)*, 13892–13902.